Frame Element with Mixed Formulations for Composite and RC Members with Bond-Slip. I: Theory and Fixed-End Rotation

Chin-Long Lee [1] and Filip C. Filippou [2]

ABSTRACT

The paper proposes a composite frame element for the simulation of the inelastic response of structural members made up of two or more components with different materials, such as reinforced concrete, steel-concrete composite members, prestressed members, and members with FRP reinforcement. The element accounts for the relative slip at the interface between the components. Nonlinear geometry effects are accounted for through the co-rotational formulation which permits the response simulation of composite frame elements under large displacements. The element formulation enhances the standard Hu-Washizu variational principle with fields describing the bond-slip behavior between components. Three alternatives for the mixed formulation of the element are derived in this paper which focuses on theory and implementation: mixed-displacement, mixed-force, and mixed-mixed. The paper presents the benefits and shortcomings of the formulation alternatives for modeling the pull-out failure of reinforcing bars and the fixed-end rotation of reinforced concrete members, and discusses the numerical ramifications of each alternative. A companion paper discusses the convergence performance of the different mixed formulations and validates the proposed element through correlation studies with available experimental results.

Keywords: Composite Element; Reinforced-Concrete Element; Frame Element; Mixed Formulation; Bond-Slip; Pull-Out Failure; Fixed-End Rotation.

[1]Dept. of Civil & Nat. Res. Eng., , Univ. of Canterbury, Private Bag 4800, Christchurch New Zealand 8140. E-mail: chin-long.lee@canterbury.ac.nz.

[2]Dept. of Civil & Environ. Eng., Univ. of California, 760 Davis Hall, Berkeley, CA 94720-1710. E-mail: filippou@ce.berkeley.edu.

INTRODUCTION

In structural members made up of two or more components with different materials, such as reinforced concrete and steel-concrete composite members, as well as members with FRP reinforcement, the bond between components is important in maintaining the composite action for strength and stiffness. The relative slip between components under service and ultimate load conditions affects the element deformation and energy dissipation capacity of the structural member and may contribute to its failure under large inelastic deformation reversals. Studies on the anchorage behavior of reinforcing bars by Eligehausen et al. (1983) and Filippou et al. (1983) found that fixed-end rotations due to reinforcing bar pull-out may contribute up to 50% of the tip displacement of a reinforced concrete cantilever column. The modeling of this effect is, therefore, important in the evaluation of the local and global response of structures under earthquake excitations.

One of the earliest reinforced concrete beam models with bond-slip under large inelastic deformation reversals was proposed by Filippou and Issa (1988), who subdivided a beam element into different subelements. The model was used later in several validation studies by Filippou et al. (1999). To account for the added flexibility due to bond-slip, Saatcioglu et al. (1992) and Rubiano-Benavides (1998) inserted nonlinear rotational springs at the beam ends. Monti and Spacone (2000) incorporated the bond-slip interaction into a fiber beam element by combining the formulation of anchored bars by Monti et al. (1997) with the beam model by Spacone et al. (1996). Subsequent studies included the bond-slip effect in frame elements with three alternative formulations: a displacement formulation (e.g. Dall'Asta and Zona, 2002, Sun and Bursi, 2005, Lin and Zhang, 2013), a force formulation (e.g. Salari et al., 1998, Salari and Spacone, 2001a;b), and a mixed formulation (e.g. Ayoub, 1999, Ayoub and Filippou, 2000, Limkatanyu and Spacone, 2002, Dall'Asta and Zona, 2004, Sun and Bursi, 2005, Ayoub, 2006). The mixed formulations use independent interpolation functions for the displacement and stress or for the displacement, the stress, and the strain field. Spacone and El-Tawil (2004) reviewed the state of the art of these three modeling approaches and concluded that the force and mixed formulations were superior to the displacement formulation in terms of accuracy and numerical robustness.

Most formulations to date interpolate the displacement or the force field, or both fields for each component of the structural member separately. The bond-slip field is then derived from the difference of the component displacement fields. While this approach is straightforward, it suffers from the following shortcomings:

1. The axial nodal displacements of each component are global degrees of freedom, so the transformation from the local to the global reference frame requires a special constraint matrix for the transverse displacements and rotations. Such a transformation is inconvenient but feasible under linear geometry. It is, however, difficult under nonlinear geometry involving large translations and rotations at the nodes.
2. The section force fields are interpolated separately for each component, so the exact interpolation of the total section force field for the entire element is not guaranteed. Without this exact interpolation, the force and mixed formulation may loose some of their advantage over the displacement formulation regarding accuracy and numerical robustness.

To address these shortcomings, this study proposes a new composite element. The element formulation is based on an extension of the Hu-Washizu variational principle and uses the exact interpolation of the total section forces of the composite element. The proposed approach treats the composite element as a single element and includes the bond-slip behavior at the interface between components at each section of the element. Consequently, the degrees of freedom for the relative slip between element components can be easily transformed between the local and the global reference frame without a constraint or special transformation matrix. Because of this advantage, this approach was adopted in some recent studies (e.g. Tort and Hajjar, 2010, Hjiaj et al., 2012), but only the formulations in this paper and in a previous study by the authors (e.g. Lee, 2008, Lee and Filippou, 2010) highlight the advantage of the exact interpolation of the total section forces for the composite element.

Based on different options for enforcing the displacement-strain compatibility condition in the bond-slip field (Lagrange relaxation), the paper presents three alternatives for the mixed formulation of the composite element: a mixed-displacement formulation with compatibility enforced in the strong form, a mixed-force formulation with equilibrium enforced in the strong form, and a mixed-mixed formulation with compatibility and equilibrium enforced in the weak form. The interpolation of the bond-slip field uses piecewise polynomials. These formulations are evaluated relative to response accuracy, numerical convergence and numerical robustness. The correlation studies with available experimental results confirm the validity of the proposed approach.

This paper presents the theoretical framework and the implementation of the proposed formulations with a discussion of the benefits and shortcomings of each formulation. The evaluation of their numerical performance and the validation studies are presented in the companion paper. Further details of the proposed element can be found in the doctoral thesis by Lee (2008).

The beam-column elements with the proposed formulations have been implemented in the Matlab® toolbox FEDEASLab (`http://fedeaslab.berkeley.edu`) that allows nonlinear structural simulations under static and transient loading (Filippou and Constantinides, 2004), and will soon be implemented in OpenSees (`http://opensees.berkeley.edu`) by Mckenna (1997).

ELEMENT FORMULATION

A new composite frame element which accounts for the bond-slip behavior at the interface between its constituent components is presented in the following. The element can be used for the simulation of the inelastic response of reinforced concrete members, prestressed concrete and timber members with straight tendons, steel-concrete composite members, concrete-filled steel tube members, and FRP-strengthened members. The element formulation is based on the three-field Hu-Washizu variational principle, as described in Taylor et al. (2003), Saritas

(2006), Lee (2008), and Lee and Filippou (2009). The standard Hu-Washizu variational principle is enhanced with additional fields to account for the bond-slip behavior at the interface between the components of the frame element.

The following general derivation assumes that the composite frame element is made up of two components with different material. The extension to an element with more components is straightforward, as will be briefly addressed after the element formulation. The presentation is limited to plane frame elements, but the extension to 3d frame elements without coupling of torsional effects is possible with an appropriate extension of the element variables and the section stress resultants.

To simplify the element formulation the following assumptions about the geometry and the deformation of the composite frame element are made:

1. the frame element is prismatic;
2. plane sections of each component remain plane and normal to the beam axis after deformation; and
3. there is no relative transverse displacement normal to the reference element between components.

The proposed formulation is thus limited to frame elements with Euler-Bernoulli kinematics for each component, and with relative displacement between components only in the direction parallel to the reference axis.

Element Displacements and Forces

The nodal forces $\mathbf{p}$ and displacements $\mathbf{u}$ of a frame element with perfect bond between components are shown in Fig. 1(a). In the presence of relative slip between components, additional degrees of freedom (DOFs) arise at the element ends, one at each end for each additional component. These additional *slip DOFs* describe the relative displacement between the components at the element ends and are denoted with u_{bI} and u_{bJ} for nodes I and J, respectively (Fig. 1(b)). The element forces at the slip DOFs are denoted with p_{bI} and p_{bJ}, in correspondence with u_{bI} and u_{bJ}, respectively. These additional displacements and forces are grouped in vectors $\mathbf{u_{bn}}$ and $\mathbf{p_{bn}}$, as follows:

$$\mathbf{u_{bn}} = \begin{bmatrix} u_{bI} & u_{bJ} \end{bmatrix}^T , \quad \mathbf{p_{bn}} = \begin{bmatrix} p_{bI} & p_{bJ} \end{bmatrix}^T \tag{1}$$

In Fig. 1(b) the white circles at the element nodes indicate additional DOFs, not additional nodes. These DOFs do not require a geometric description, because they are associated with the element nodes. Fig. 1(b) shows the relative DOFs in the deformed state following a relative translation of $\mathbf{u_{bn}}$.

Each slip value in $\mathbf{u_{bn}}$ is a *relative* DOF between the two components at the node, and its direction is a *local* property. At the initial state, the direction of each slip DOF is tangent to the y-coordinate profile of the interface between the two components. When the element node rotates with deformation, the direction of the slip DOF follows the rotation and remains in the direction of the node tangent (Fig. 1(b)), even for a non-prismatic frame element. Because of displacement compatibility at the common node of two elements, the direction of $\mathbf{u_{bn}}$ is the same after deformation. This obviates the need for a transformation matrix for the slip DOFs from the local to the global reference system, and the slip DOF increments during the iterative solution of the global equilibrium equations are determined in the local reference system. This holds true even under nonlinear geometry as long as the co-rotational formulation is used for large displacement analysis, making the proposed frame element with slip DOFs easy to implement in a general purpose finite element analysis program for large displacement analysis, a feature that distinguishes this element from earlier proposals of composite frame elements.

Section Kinematics

Figure 2 shows the general cross-section of the structural member with two components and the general displacement profile u in the x-direction. In the following presentation, the variables referring to components 1 and 2 are denoted with subscripts 1 and 2, respectively.

As shown, the interface between the two components need not be planar. In agreement with the assumption of Euler-Bernoulli kinematics, the displacement field of the section with perfect bond can be written in terms of the axial displacement u_a at the reference axis and the derivative of the lateral displacement u_y as

$$u(x,y) = u_a(x) - y\,u_y'(x) = \mathbf{a_u}\mathbf{u}_s(x) + \mathbf{a}_{\boldsymbol{\theta}}(y)\,\mathbf{u}_s'(x) \tag{2}$$

With a prime denoting differentiation with respect to x, $\mathbf{a_u}$ and $\mathbf{a}_{\boldsymbol{\theta}}$ are displacement interpolation matrices and $\mathbf{u}_s$ are the section displacements whereby

$$\mathbf{a_u} = \begin{bmatrix} 1 & 0 \end{bmatrix}, \quad \mathbf{a}_{\boldsymbol{\theta}} = \begin{bmatrix} 0 & -y \end{bmatrix}, \quad \mathbf{u}_s = \begin{bmatrix} u_a & u_y \end{bmatrix}^T \tag{3}$$

In the presence of *relative slip* u_b of component 2 with respect to component 1, the displacement field of the section becomes (Figure 2)

$$u(x,y) = \mathbf{a_u}\,\mathbf{u}_s(x) + \mathbf{a}_{\boldsymbol{\theta}}(y)\,\mathbf{u}_s'(x) + a_b\,u_b(x) \tag{4}$$

where a_b takes on the value 0 and 1 for components 1 and 2, respectively.

The strain field ε^u for this displacement field is

$$\varepsilon^u(x,y) = \mathbf{a_u}\mathbf{u}_s'(x) + \mathbf{a}_{\boldsymbol{\theta}}(y)\mathbf{u}_s''(x) + a_b u_b'(x) \tag{5}$$

Eq. (5) shows that the strain difference of the two components is the derivative of the relative slip u_b. This difference defines the *slip strain* ε_b, which depends on x only and is given by

$$\varepsilon_b(x) = u_b'(x) \tag{6}$$

In the following the material strain in component 1 is denoted with ε and the material strain in component 2 is expressed as the sum of ε and ε_b.

Variational Principle

For a frame element with uniaxial material response and volume $\Omega = A \times [0, L]$, the functional for the standard Hu-Washizu variational principle is (Lee and Filippou, 2009)

$$\Pi\left[(\mathbf{u}_s, \mathbf{u}), \sigma, \varepsilon\right] = \int_\Omega W(\varepsilon)\, d\Omega - \int_0^L \mathbf{u}_s^T \bar{\mathbf{w}}\, dx - \mathbf{u}^T \mathbf{p} + \int_\Omega \sigma(\varepsilon^u(\mathbf{u}_s) - \varepsilon)\, d\Omega \tag{7}$$

The function W is the energy density function which permits the determination of the material stress σ according to $\hat{\sigma}(\varepsilon) = \partial W/\partial \varepsilon$. The element loading $\bar{\mathbf{w}}$ consists of a uniformly distributed axial load $\bar{w}_x$ and a uniformly distributed transverse load $\bar{w}_y$.

In the presence of partial bond between the two components, the functional Π can be enhanced with an additional functional Π_b that describes the bond interaction at the interface of the two components with contact area $A_b = p_b \times [0, L]$, where p_b is the perimeter of component 2 in contact with component 1. The functional Π_b is given by

$$\Pi_b\left[(u_b, \mathbf{u_{bn}}), \sigma_2, \varepsilon_b\right] = \int_{A_b} W_b(u_b)\, dA - \mathbf{u_{bn}}^T \bar{\mathbf{p}}_{\mathbf{bn}} + \int_{\Omega_2} \sigma_2(u_b' - \varepsilon_b)\, d\Omega \tag{8}$$

where W_b is the energy density function which permits the determination of the bond stress σ_b according to $\hat{\sigma}_b(u_b) = \partial W_b/\partial u_b$. The last term in Eq. (8) is the Lagrange multiplier enforcing strain compatibility in component 2, where Ω_2 is the volume of component 2. With the inclusion of partial bond, the energy density function W in Π also depends on ε_b, so that $W(\varepsilon, \varepsilon_b)$.

Interpolation Functions

If the strain ε_b in W is held fixed, the functional Π involves only three independent fields: the displacements ($\mathbf{u}_s$,$\mathbf{u}$), the material stress σ and the material strain ε. These can be interpolated from the nodal displacements $\mathbf{u}$, the basic element forces $\mathbf{q}$ and element loads

$\bar{\mathbf{w}}$, and the section deformations $\mathbf{e}$ according to

$$
\begin{aligned}
\mathbf{u}_s(x) &= \mathbf{a}_{\mathbf{us}}(x)\mathbf{u} && \text{(9a)}\\
\sigma(x,y) &= \mathbf{b}_{\mathbf{s}}(y)\mathbf{s}(x), \quad \mathbf{s}(x) = \mathbf{b}(x)\mathbf{q} + \bar{\mathbf{s}}_{\mathbf{w}}(x), \quad \bar{\mathbf{s}}_{\mathbf{w}}(x) = \mathbf{b}_{\mathbf{w}}(x)\bar{\mathbf{w}} && \text{(9b)}\\
\varepsilon(x,y) &= \mathbf{a}_{\mathbf{s}}(y)\mathbf{e}(x) && \text{(9c)}
\end{aligned}
$$

where $\mathbf{a}_{\mathbf{us}}$, $\mathbf{b}_{\mathbf{s}}$, $\mathbf{b}$, $\mathbf{b}_{\mathbf{w}}$ and $\mathbf{a}_{\mathbf{s}}$ are interpolation matrices. The basic element forces $\mathbf{q}$ for the plane frame element are the axial force q_1 and the two end moments q_2 and q_3. The section deformations $\mathbf{e}$ consist of the axial strain ε_a at the element axis and the curvature κ. The section forces $\mathbf{s}$ consist of the axial force N and the bending moment M.

The interpolation functions $\mathbf{b}$ and $\mathbf{b}_{\mathbf{w}}$ are

$$
\mathbf{b}(x) = \begin{bmatrix} 1 & 0 & 0 \\ 0 & x/L - 1 & x/L \end{bmatrix}, \quad \mathbf{b}_{\mathbf{w}}(x) = \begin{bmatrix} L - x & 0 \\ 0 & x(x-L)/2 \end{bmatrix} \tag{10}
$$

Because these interpolation functions satisfy the differential equilibrium equations of the plane frame element in the undeformed configuration

$$
N'(x) + \bar{w}_x = 0, \quad M''(x) - \bar{w}_y = 0 \tag{11}
$$

the interpolation functions $\mathbf{a}_{\mathbf{us}}$ are not necessary in the element formulation in a reference system without rigid body modes (Taylor et al., 2003, Saritas, 2006, Lee and Filippou, 2009). The interpolation functions $\mathbf{a}_{\mathbf{s}}$ that satisfy the section kinematics are given by

$$
\mathbf{a}_{\mathbf{s}}(y) = \begin{bmatrix} 1 & -y \end{bmatrix} \tag{12}
$$

The interpolation functions $\mathbf{b}_{\mathbf{s}}$ are given by

$$
\mathbf{b}_{\mathbf{s}}(y) = \mathbf{a}_{\mathbf{s}}(y) \left(\int_A \mathbf{a}_{\mathbf{s}}(y)^T \mathbf{a}_{\mathbf{s}}(y)\, dA \right)^{-1} = \begin{bmatrix} 1/A & -y/I \end{bmatrix} \tag{13}
$$

where I is the second moment of area. The inverse in Eq. (13) is well-defined because the columns of $\mathbf{a_s}$ are independent of each other over the cross-section A. The interpolation functions $\mathbf{b_s}$ are selected to satisfy the following relation (Lee and Filippou, 2009):

$$\int_A \mathbf{a_s}(y)^T \mathbf{b_s}(y)\, dA = \mathbf{I} \tag{14}$$

where $\mathbf{I}$ is the identity matrix.

The substitution of the above interpolation functions with integration by parts and some simplifications transforms the functional Π to

$$\begin{aligned} \Pi(\mathbf{u}, \mathbf{q}, \mathbf{e}, \varepsilon_b) = \int_0^L W_s(\mathbf{e}, \varepsilon_b)\, dx - \int_0^L \bar{\mathbf{s}}_{\mathbf{w}}^T \mathbf{e}\, dx - \mathbf{u}^T (\bar{\mathbf{p}}_{\mathbf{w}} + \bar{\mathbf{p}}) \\ + \mathbf{q}^T \left(\mathbf{a}\mathbf{u} - \int_0^L \mathbf{b}^T \mathbf{e}\, dx \right) \end{aligned} \tag{15}$$

where $\bar{\mathbf{p}}_{\mathbf{w}}$ are the element nodal forces arising from $\bar{\mathbf{w}}$ and given by

$$\bar{\mathbf{p}}_{\mathbf{w}} = \begin{bmatrix} \bar{w}_x L & \bar{w}_y L/2 & 0 & 0 & \bar{w}_y L/2 & 0 \end{bmatrix}^T \tag{16}$$

and $\mathbf{a}$ is the rigid body mode transformation matrix given by

$$\mathbf{a} = \begin{bmatrix} -1 & 0 & 0 & 1 & 0 & 0 \\ 0 & 1/L & 1 & 0 & -1/L & 0 \\ 0 & 1/L & 0 & 0 & -1/L & 1 \end{bmatrix} \tag{17}$$

The energy W_s is the section energy density function defined as

$$W_s(\mathbf{e}, \varepsilon_b) = \int_A W(\mathbf{a_s}\mathbf{e}, \varepsilon_b)\, dA \tag{18}$$

which permits the determination of the section forces $\mathbf{s}$ from $\hat{\mathbf{s}}(\mathbf{e}, \varepsilon_b) = \partial W_s / \partial \mathbf{e}$ as well as the determination of the axial force of component 2 from $\hat{N}_2(\mathbf{e}, \varepsilon_b) = \partial W_s / \partial \varepsilon_b$.

The functional Π_b also has three independent fields: the displacements u_b and $\mathbf{u_{bn}}$, the material stress σ_2 of component 2, and the slip strain ε_b. Depending on the way the relation between u_b and ε_b is established three alternative expressions are possible for Π_b. Each alternative leads to a different formulation for the frame element, as will be discussed in the next section. The functional Π_b is first rewritten as follows:

$$\Pi_b((u_b, \mathbf{u_{bn}}), \sigma_2, \varepsilon_b) = \int_0^L W_{sb}(u_b)\, dx - \mathbf{u_{bn}}^T \bar{\mathbf{p}}_{\mathbf{bn}} + \int_{\Omega_2} \sigma_2(u_b' - \varepsilon_b)\, d\Omega \tag{19}$$

where $W_{sb}(u_b) = \int_{p_b} W_b(u_b)\, ds$ is the energy density function that permits the determination of bond force N_b from $\hat{N}_b(u_b) = \partial W_{sb}/\partial u_b$.

New Variational Formulations

The variation of Π with respect to $\mathbf{u}$, $\mathbf{q}$ and $\mathbf{e}$ under a fixed value ε_b leads to three governing equations for a 2d Euler-Bernoulli beam element (Lee and Filippou, 2009):

$$\mathbf{R_p}(\mathbf{q}) = \mathbf{a}^T\mathbf{q} - \bar{\mathbf{p}} - \bar{\mathbf{p}}_{\mathbf{w}} = \mathbf{0} \tag{20a}$$

$$\mathbf{R_v}(\mathbf{u}, \mathbf{e}) = \mathbf{a}\mathbf{u} - \sum_{l=1}^{N_p} \mathbf{b}_l^T \mathbf{e}_l\, w_l = \mathbf{0} \tag{20b}$$

$$\mathbf{R}_{\mathbf{s}l}(\mathbf{q}, \mathbf{e}_l, \varepsilon_b) = \hat{\mathbf{s}}_l(\mathbf{e}_l, \varepsilon_b) w_l - (\mathbf{b}_l\mathbf{q} + \bar{\mathbf{s}}_{\mathbf{w}l}) w_l = \mathbf{0} \quad \text{(for each section } l\text{)} \tag{20c}$$

The first equation in Eq. (20) is transformed to the global reference system with the corotational formulation (Felippa and Haugen, 2005, Le Corvec, 2012) before assembly of the resisting force vector for the structural model. The other two equations in Eq. (20) are local and can be condensed out during the state determination process of the frame element, as discussed in Lee and Filippou (2009).

The additional governing equations resulting from Π_b are derived next. Because ε_b is an independent variable for both functionals Π and Π_b, the first variation of these functionals with respect to ε_b results in the coupling of the two sets of governing equations. The governing equations arising from Π_b depend on the relation between u_b and ε_b. Three formulations for the bond-slip field of the composite element are possible: mixed-displacement (MD), mixed-mixed (MM), and mixed-force (MF) formulations. The first word "mixed" refers to the Hu-Washizu variational principle that furnishes the framework for the formulation. The second word refers to the option of interpolating the relative slip u_b (displacement), or the axial force of the second component N_2 (force), or the option of interpolating both fields (mixed).

Mixed-Displacement (MD) Formulation

In the mixed-displacement (MD) formulation, the slip strain ε_b is point-wise equal to the first derivative of the relative slip u_b. Under this condition the third term of Π_b, serving as Lagrange multiplier, vanishes. The derivative of u_b thus replaces the argument ε_b of W_s. With the assumption of a generalized slip $\mathbf{u_b}$ and an interpolation matrix $\mathbf{a_b}$ along the x-axis for u_b, the fields of u_b and ε_b can be expressed as

$$u_b(x) = \mathbf{a_b}(x)\mathbf{u_b}, \quad \varepsilon_b(x) = \mathbf{a_{bx}}(x)\mathbf{u_b} \tag{21}$$

where the interpolation matrix $\mathbf{a_{bx}}$ is the derivative of $\mathbf{a_b}$ with respect to x. The nodal slip values $\mathbf{u_{bn}}$ correspond to the values of the u_b field at the end sections of the composite element given by

$$\mathbf{u_{bn}} = \mathbf{a_{bn}}\mathbf{u_b} \tag{22}$$

where

$$\mathbf{a_{bn}} = \begin{bmatrix} \mathbf{a_b}(0) \\ \mathbf{a_b}(L) \end{bmatrix} \tag{23}$$

With these interpolation functions the functional Π_b becomes

$$\Pi_b(\mathbf{u_b}) = \int_0^L W_{sb}(\mathbf{a_b}\mathbf{u_b})\, dx - \mathbf{u_b}^T(\mathbf{a_{bn}}^T\bar{\mathbf{p}}_{\mathbf{bn}}) \tag{24}$$

after the substitution of Eq. (21). The first variation of Eqs. (15) and (24) with respect to $\mathbf{u_b}$ gives the following governing equation

$$\mathbf{R_b}(\mathbf{u_b}, \mathbf{e}) = \hat{\mathbf{N}}_\mathbf{a} + \hat{\mathbf{N}}_\mathbf{b} - \mathbf{a_{bn}}^T \bar{\mathbf{p}}_\mathbf{bn} = \mathbf{0} \tag{25}$$

where

$$\hat{\mathbf{N}}_\mathbf{a} = \int_0^L \mathbf{a_{bx}}^T \hat{N}_2 \, dx, \quad \hat{\mathbf{N}}_\mathbf{b} = \int_0^L \mathbf{a_b}^T \hat{N}_b \, dx \tag{26}$$

Eqs. (20) and (25) form the governing equations of the mixed-displacement (MD) formulation.

Mixed-Mixed (MM) Formulation

In the mixed-mixed (MM) formulation, the Lagrange term is retained as the penalty form of strain-displacement compatibility along the element. The presence of the penalty term requires the interpolation of the material stress field σ_2 in addition to the relative slip field u_b. It is assumed that the axial force field N_2 of component 2 can be expressed in terms of the generalized forces $\mathbf{q_b}$ such that

$$N_2(x) = \mathbf{b_b}(x)\mathbf{q_b} \tag{27}$$

where $\mathbf{b_b}$ is the corresponding force interpolation matrix. The material stress σ_2 is the average of force N_2 over the cross-sectional area A_2 of component 2:

$$\sigma_2(x, y) = \frac{N_2(x)}{A_2} = \frac{1}{A_2}\mathbf{b_b}(x)\mathbf{q_b} \tag{28}$$

The forces $\mathbf{q_b}$ are local element variables so that no inter-element continuity at the nodes is required and these variables can be condensed out at the element level without introducing additional global degrees-of-freedom. Upon substitution of the above interpolation function for σ_2 and the interpolation function for u_b in Eq. (21), the functional Π_b in Eq. (19) becomes:

$$\Pi_b(\mathbf{u_b}, \mathbf{q_b}, \varepsilon_b) = \int_0^L W_{sb}(\mathbf{a_b}\mathbf{u_b})\, dx - \mathbf{u_b}^T \mathbf{a_{bn}}^T \bar{\mathbf{p}}_{\mathbf{bn}} + \mathbf{q_b}^T \left(\mathbf{a_{bm}}\mathbf{u_b} - \int_0^L \mathbf{b_b}^T \varepsilon_b \, dx \right) \quad (29)$$

where

$$\mathbf{a_{bm}} = \int_{\Omega_2} \frac{1}{A_2} \mathbf{b_b}^T \mathbf{a_{bx}}\, d\Omega = \int_0^L \mathbf{b_b}^T \mathbf{a_{bx}}\, dx \quad (30)$$

As discussed by Ayoub and Filippou (1999; 2000), the stability of this formulation requires that the number of unknowns n_q in $\mathbf{q_b}$ and the number of unknowns n_u in $\mathbf{u_b}$ satisfy the following condition:

$$n_q \geq n_u - 1 \quad (31)$$

183 Under this condition a linear polynomial is required for the force field N_2, if a quadratic
184 polynomial is selected for the relative slip field u_b.

The functional Π_b in Eq. (29) is similar to the functional Π in Eq. (15), except that the internal energy of Π_b depends on u_b, whereas the internal energy of Π depends on ε and ε_b. It is, therefore, natural to combine these functionals into a single expression. To do this, the two sets of variables are stacked on top of each other to form new vectors, which are defined below with some abuse of notation

$$\mathbf{u} \Leftarrow \begin{bmatrix} \mathbf{u} \\ \mathbf{u_b} \end{bmatrix}, \quad \mathbf{q} \Leftarrow \begin{bmatrix} \mathbf{q} \\ \mathbf{q_b} \end{bmatrix}, \quad \mathbf{e} \Leftarrow \begin{bmatrix} \mathbf{e} \\ \varepsilon_b \end{bmatrix} \quad (32a)$$

$$\mathbf{a} \Leftarrow \begin{bmatrix} \mathbf{a} & \mathbf{0} \\ \mathbf{0} & \mathbf{a_{bm}} \end{bmatrix}, \quad \mathbf{a_b} \Leftarrow \begin{bmatrix} \mathbf{0} & \mathbf{a_b} \end{bmatrix}, \quad \mathbf{b} \Leftarrow \begin{bmatrix} \mathbf{b} & \mathbf{0} \\ \mathbf{0} & \mathbf{b_b} \end{bmatrix}, \quad \mathbf{a_s} \Leftarrow \begin{bmatrix} \mathbf{a_s} & a_b \end{bmatrix} \quad (32b)$$

$$\bar{\mathbf{p}} \Leftarrow \begin{bmatrix} \bar{\mathbf{p}} \\ \mathbf{a_{bn}}^T \bar{\mathbf{p}}_{\mathbf{bn}} \end{bmatrix}, \quad \bar{\mathbf{p}}_{\mathbf{w}} \Leftarrow \begin{bmatrix} \bar{\mathbf{p}}_{\mathbf{w}} \\ \mathbf{0} \end{bmatrix}, \quad \bar{\mathbf{s}}_{\mathbf{w}} \Leftarrow \begin{bmatrix} \bar{\mathbf{s}}_{\mathbf{w}} \\ 0 \end{bmatrix} \quad (32c)$$

The functional for the mixed-mixed (MM) formulation then becomes

$$\Pi_m(\mathbf{u},\mathbf{q},\mathbf{e}) = \int_0^L W_{sm}(\mathbf{e})\,dx + \int_0^L W_{sb}(\mathbf{a_b}\mathbf{u})\,dx - \int_0^L \bar{\mathbf{s}}_{\mathbf{w}}^T\mathbf{e}\,dx - \mathbf{u}^T(\bar{\mathbf{p}}_{\mathbf{w}} + \bar{\mathbf{p}}) + \mathbf{q}^T\left(\mathbf{a}\mathbf{u} - \int_0^L \mathbf{b}^T\mathbf{e}\,dx\right) \tag{33}$$

The energy density function W_{sm} is equivalent to W_s in Eq. (18) except that the argument ε_b in W_s is grouped into the argument $\mathbf{e}$ in W_{sm}. Hence, the section forces $\hat{\mathbf{s}}$ from W_{sm} have three components: the first two components are the axial force $\hat{N}$ and bending moment $\hat{M}$ of the element, as for the standard formulation, whereas the third component is the axial force $\hat{N}_2$ of component 2. The element forces from the energy density function W_{sb} are

$$\hat{\mathbf{p}}_{\mathbf{b}}(\mathbf{u}) = \int_0^L \frac{\partial W_{sb}}{\partial \mathbf{u}}\,dx = \begin{bmatrix} \mathbf{0} \\ \hat{\mathbf{N}}_{\mathbf{b}}(\mathbf{u_b}) \end{bmatrix} \tag{34}$$

The functional Π_m in Eq. (33) has exactly the same form as the functional in Eq. (15), except that Π_m contains an additional internal energy term that depends on the displacement field. The first variation of Π_m gives the following governing equations for the MM formulation:

$$\mathbf{R}_{\mathbf{p}}(\mathbf{u},\mathbf{q}) = \mathbf{a}^T\mathbf{q} + \hat{\mathbf{p}}_{\mathbf{b}}(\mathbf{u}) - \bar{\mathbf{p}} - \bar{\mathbf{p}}_{\mathbf{w}} = \mathbf{0} \tag{35a}$$

$$\mathbf{R}_{\mathbf{v}}(\mathbf{u},\mathbf{e}) = \mathbf{a}\mathbf{u} - \sum_{l=1}^{N_p} \mathbf{b}_l^T\mathbf{e}_l\,w_l = \mathbf{0} \tag{35b}$$

$$\mathbf{R}_{\mathbf{s}l}(\mathbf{q},\mathbf{e}_l) = \hat{\mathbf{s}}_l(\mathbf{e}_l)w_l - (\mathbf{b}_l\mathbf{q} + \bar{\mathbf{s}}_{\mathbf{w}l})w_l = \mathbf{0} \quad \text{(for each section } l\text{)} \tag{35c}$$

The governing equations in Eq. (35) have the same form as the original three governing equations, except that the first equation now includes the resisting forces $\hat{\mathbf{p}}_{\mathbf{b}}$ at the interface of the element components that depend on the displacement field $\mathbf{u}$.

Mixed-Force (MF) Formulation

In the mixed-force (MF) formulation the Lagrange multiplier term in Eq. (19) is modified by interpolating the material stress σ_2 according to Eq. (28) such that

$$\int_{\Omega_2} \sigma_2(u_b' - \varepsilon_b)\, d\Omega = \mathbf{q_b}^T \int_0^L \mathbf{b_b}^T (u_b' - \varepsilon_b)\, dx \tag{36}$$

After integration by parts Eq. (36) becomes

$$\int_{\Omega_2} \sigma_2(u_b' - \varepsilon_b)\, d\Omega = \mathbf{q_b}^T \left(\mathbf{a_{bf}} \mathbf{u_{bn}} - \int_0^L (\mathbf{b_b}^T \varepsilon_b + \mathbf{b_{bx}}^T u_b)\, dx \right) \tag{37}$$

where $\mathbf{b_{bx}}$ is the derivative of $\mathbf{b_b}$ with respect to x, and

$$\mathbf{a_{bf}} = \begin{bmatrix} -\mathbf{b_b}^T(0) & \mathbf{b_b}^T(L) \end{bmatrix} \tag{38}$$

Substituting Eq. (37) into Eq. (19) results in the following functional Π_b

$$\begin{aligned} \Pi_b((u_b, \mathbf{u_{bn}}), \sigma_2, \varepsilon_b) = & \int_0^L W_{sb}(u_b)\, dx - \mathbf{u_{bn}}^T \bar{\mathbf{p}}_{\mathbf{bn}} \\ & + \mathbf{q_b}^T \left(\mathbf{a_{bf}} \mathbf{u_{bn}} - \int_0^L (\mathbf{b_b}^T \varepsilon_b + \mathbf{b_{bx}}^T u_b)\, dx \right) \end{aligned} \tag{39}$$

In this functional the variables u_b and $\mathbf{u_{bn}}$ are independent of each other because they are defined at different points of the frame element axis. The variable u_b is defined in the element interior, while $\mathbf{u_{bn}}$ denotes the slip value at the end sections of the element. Inter-element continuity is imposed on $\mathbf{u_{bn}}$, but not on u_b, which is, therefore, a local element variable that can be condensed out during the state determination.

The functional Π_b in Eq. (39) is similar to the functional Π in Eq. (15). As is the case for the MM formulation, these two functionals can be combined by stacking the independent variables of Π on top of the independent variables of Π_b. With an abuse of notation, the new vectors are listed below without section variables:

$$\mathbf{u} \Leftarrow \begin{bmatrix} \mathbf{u} \\ \mathbf{u_{bn}} \end{bmatrix}, \qquad \mathbf{q} \Leftarrow \begin{bmatrix} \mathbf{q} \\ \mathbf{q_b} \end{bmatrix} \tag{40a}$$

$$\mathbf{a} \Leftarrow \begin{bmatrix} \mathbf{a} & \mathbf{0} \\ \mathbf{0} & \mathbf{a_{bf}} \end{bmatrix} \tag{40b}$$

$$\bar{\mathbf{p}} \Leftarrow \begin{bmatrix} \bar{\mathbf{p}} \\ \bar{\mathbf{p}}_{\mathbf{bn}} \end{bmatrix}, \quad \bar{\mathbf{p}}_{\mathbf{w}} \Leftarrow \begin{bmatrix} \bar{\mathbf{p}}_{\mathbf{w}} \\ \mathbf{0} \end{bmatrix} \tag{40c}$$

The section variables are combined separately for the two sections of the model: the first section, subsequently called fiber section, refers to the cross section of the element that is discretized into fibers so that its response results from the integration of the uniaxial material response. This cross section is the aggregation of the component sections. With an abuse of notation the section variables and interpolation matrices are

$$\mathbf{e} \Leftarrow \begin{bmatrix} \mathbf{e} \\ \varepsilon_b \end{bmatrix}, \quad \mathbf{a_s} \Leftarrow \begin{bmatrix} \mathbf{a_s} & a_b \end{bmatrix}, \quad \mathbf{b} \Leftarrow \begin{bmatrix} \mathbf{b} & \mathbf{0} \\ \mathbf{0} & \mathbf{b_b} \end{bmatrix}, \quad \bar{\mathbf{s}}_{\mathbf{w}} \Leftarrow \begin{bmatrix} \bar{\mathbf{s}}_{\mathbf{w}} \\ 0 \end{bmatrix} \tag{41}$$

The second section, subsequently called *interface section*, refers to section variables at the interface between the element components. The force resultants of the interface section arise from bond stresses. With an abuse of notation these section variables and interpolation matrices are

$$\mathbf{e} \Leftarrow u_b, \quad \mathbf{b} \Leftarrow \begin{bmatrix} \mathbf{0} & \mathbf{b_{bx}} \end{bmatrix}, \quad \bar{\mathbf{s}}_{\mathbf{w}} \Leftarrow 0 \tag{42}$$

With the new set of variables and the two sets of section force resultants, the functional for the MF formulation becomes

$$
\begin{aligned}
\Pi_f(\mathbf{u}, \mathbf{q}, \mathbf{e}) = \int_0^L W_{sf}(\mathbf{e})\, dx - \int_0^L \bar{\mathbf{s}}_{\mathbf{w}}^T \mathbf{e}\, dx - \mathbf{u}^T(\bar{\mathbf{p}}_{\mathbf{w}} + \bar{\mathbf{p}}) \\
+ \mathbf{q}^T \left(\mathbf{a}\mathbf{u} - \int_0^L \mathbf{b}^T \mathbf{e}\, dx \right)
\end{aligned}
\tag{43}
$$

where W_{sf} is the section energy density function defined as

$$
W_{sf}(\mathbf{e}) = \begin{cases} W_{sm}(\mathbf{e}) & \text{for the fiber section} \\ W_{sb}(\mathbf{e}) & \text{for the interface section} \end{cases}
\tag{44}
$$

W_{sm} is the same energy density function as in the MM formulation. The functional W_{sf} permits the determination of the section forces $\hat{\mathbf{s}}$ from $\mathbf{e}$ with $\hat{\mathbf{s}}(\mathbf{e}) = \partial W_{sf}/\partial \mathbf{e}$. The section forces for the fiber section consist of the axial force $\hat{N}$, the bending moment $\hat{M}$, and the axial force $\hat{N}_2$, as defined for the MM formulation. The forces for the interface section consist of the bond force $\hat{N}_b$ at the interface of the composite frame element components.

Eq. (43) shows that the functional for the MF formulation has the same expression as the original functional Π in Eq. (7). The expressions of the governing equations are the same as Eq. (20), except that ε_b is grouped into $\mathbf{e}$ in Eq. (20c).

In the MF formulation the generalized bond forces $\mathbf{q_b}$ are local without requiring inter-element continuity. Nonetheless, C^0 continuity results for $\mathbf{q_b}$ through node equilibrium, because the slip values $\mathbf{u_{bn}}$ are only defined at the element nodes.

Remark 1 The proposed formulations can be used for modeling the anchorage zone of a reinforcing bar by removing the concrete component. In such case, these formulations are identical with the displacement, mixed and force formulations proposed by Ayoub and Filippou (1999). □

Remark 2 The proposed formulations can be extended to an element with multiple components that slip relative to component 1 only, *without bond-slip interaction among them.*

Each component slipping relative to component 1 gives rise to a pair of $\mathbf{u_{bn}}$ and $\mathbf{p_{bn}}$ at the end nodes, one set of u_b, ε_b and σ values for describing the slip, strain and stress fields, respectively, and, hence, one functional Π_b in Eq. (19). Since there is no bond-slip interaction among these components, their variables are uncoupled and interact only with the variables of component 1. Consequently, the governing equations for MD, MM and MF formulations remain the same (see Eqs. (20), (25) and (35)), except that each component has its own generalized slip $\mathbf{u_b}$ and force $\mathbf{q_b}$ with interpolation functions $\mathbf{a_b}$ and $\mathbf{b_b}$, respectively. For the MM and MF formulations, the variables of each component are also stacked on top of each other according to Eqs. (32), (40), (41) and (42) without coupling of the interpolation functions for these components. □

Interpolation Functions

Except for homogeneous frame elements with linear elastic materials, it is not possible to use simple exponentials or polynomials for the distribution of u_b and N_2 along the element. For representing inhomogeneous inelastic response within the element with sufficient accuracy, this study makes use of piecewise polynomials as interpolation functions for u_b and N_2 without dividing the element into sub-elements. This option balances the accuracy requirements for u_b and N_2 with the efficiency requirement of interpolating the section forces N and M with the smallest number of parameters, i.e. the use of constant and linear interpolation functions for N and M, respectively. For the mixed-displacement formulation, piecewise quadratic polynomials are used for the interpolation of u_b. For the mixed-force formulation, piecewise quadratic polynomials are used for the interpolation of N_2. Finally, for the mixed-mixed formulation, quadratic splines and linear splines are used for the interpolation of u_b and N_2, respectively. Fig. 3 illustrates these interpolation functions over a four segment portion of the composite beam. In the following, the term *segment* refers to the interval within the composite element with a well-defined polynomial.

For an optimum balance of efficiency and accuracy, linear and quadratic splines were also considered as the interpolation functions for the mixed-displacement and the mixed-force formulations, and discontinuous piecewise linear and piecewise quadratic polynomials were considered for the mixed-mixed formulation, but their evaluation falls outside the scope of this paper. Details of this evaluation are available in the Ph.D. thesis of Lee (2008).

COMPARISON OF FORMULATIONS

The following discussion addresses the advantages and limitations of the three proposed alternatives of the mixed formulation for modeling the bond-slip effect of composite frames, and in particular, the bond-slip of reinforcing bars in reinforced-concrete members.

A reinforced concrete cantilever column is used for this purpose. The column corresponds to the specimen by Bousias et al. (1995), but is used here without reference to the experimental results with the correlation studies deferred to the companion paper.

The column is 1490 mm long with a 250×250 mm square cross-section, as shown in Fig. 4, It has eight reinforcing bars (rebars) of 16 mm bar diameter uniformly distributed around the perimeter and anchored in a concrete block with an anchorage length of 30 bar diameters.

This specimen is selected because of the presence of 8 rebars in the cross section, which the proposed model can monitor independently, a feature not available in earlier models. The determination of the crack opening at the base of the column and the corresponding fixed-end rotation constitute important aspects of the evaluation of the formulation alternatives.

The column is subjected to an incremental horizontal translation at its tip to a maximum lateral drift ratio of 6% under a constant axial compressive force of 300 kN.

The compressive strength of concrete f'_c is 30.75 MPa. The model uses Mander's model (Mander et al., 1988) for the concrete stress-strain relation with no tensile resistance and a confinement factor of K=1.25 based on the reinforcement details. The analysis assumes that the entire cross section is confined, since this has little bearing on the discussion about the merits of the formulation alternatives. The model uses the general Menegotto-Pinto (GMP) model (Menegotto and Pinto, 1973) modified by Filippou et al. (1983) for the reinforcing steel with yield strength f_y of 460 MPa, Young's modulus E_s of 210 GPa, and hardening ratio of 1.4%. The model uses a trilinear bond-slip relation defined by the value-pairs of (0.25 mm, 7.9 MPa), (1 mm, 13.5 MPa) and (3 mm, 13.6 MPa), following recommendations for typical conditions in the literature (Eligehausen et al., 1983). The trilinear model is similar to the Hysteretic model in OpenSees (`http://opensees.berkeley.edu`). The bond-slip relation does not have a softening branch, since the softening behavior has no bearing on the present discussion.

The model uses one composite element for the reinforced-concrete column. Since the column is subjected to uniaxial bending with axial force, the rebars are grouped in layers according to their y-distance from the reference axis, and one component is used each group in the column element. A separate anchored bar element is used for each rebar group in the foundation. The column cross-section is subdivided into 60 layers and midpoint integration is used for the evaluation of the stress resultants. The boundary conditions of the model restrain the horizontal translation and the rotation at the column base. At the column tip the horizontal translation is controlled with the specified displacement history, and the vertical translation and rotation are free. The slip DOFs of the column element are assumed to be free at the column tip and are connected to the anchored bars at the column base. The stress of the anchored bars is set to zero at the anchorage end.

The monotonic response for the column measured by Bousias et al. (1995) does not show softening for the range of inelastic deformations of the numerical study. Nonetheless, it is important to select the segment number of the composite frame element under consideration of response objectivity. Consequently, two segments with three integration points are used to ensure that the response evaluation is exact for a linear elastic frame element without element loads. For the bond-slip field in the MF formulation, only two integration points are necessary. Moreover, the segment lengths within the composite frame element are selected in the ratio of 1 to 2, with the shortest segment closest to the column base so as to capture the rapid increase of local strains at this location. A similar segment length distribution is used for the anchored bar elements in the foundation. A general solution for objective response will be explored in the future following earlier studies for reinforced concrete frame elements without bond-slip (Coleman and Spacone, 2001, Scott and Fenves, 2006).

The top figures of Fig. 5 show the steel strain distribution, while the bottom figures show the relative slip of the reinforcement along the column and along the anchorage length of the rebars at the maximum drift ratio of 6%. The numerical results for the MD and MM formulation are shown in the figures on the left hand side, and the results for the MF formulation on the right hand side of Fig. 5. The results lead to the following observations:

Both MD and MM formulations require C^0 continuity of the slip field u_b which needs to be continuous across elements but need not have a continuous derivative. The MF formulation, on the other hand, does not impose a continuity requirement on the relative slip field u_b. Consequently, the MF formulation is much more suitable than the MD or MM formulation for modeling the discrete crack that arises between beam and column elements or between column and foundation elements as a result of bond-slip. This crack is in fact the manifestation of the discontinuous nature of relative slip across the common node of two elements and has been observed in many tests of RC columns with pull-out of the reinforcing bars from the foundation. By imposing relative slip continuity at the crack the MD and MM formulation underestimate the bar pull-out value but also lead to discrepancies for the relative slip distribution in the element that pulls out.

All formulations do not enforce inter-element continuity for the axial force of component 2, but only the MF formulation establishes force continuity at the element nodes through node equilibrium. In the example of the reinforcing bar pull-out for a cantilever RC column, the equilibrium requires that the reinforcing steel stress be continuous across the column-foundation interface. Both MD and MM formulations fail to capture this continuity correctly. By contrast, the MF formulation, which accommodates the continuity of the steel force at the column base, produces better results for the stress in the reinforcing steel, as the correlation studies of the companion paper demonstrate.

In conclusion, the MF formulation is the best formulation for simulating pull-out of the reinforcement of one element from its anchorage in another element since it represents the discontinuous slip across the common node.

ESTIMATION OF FIXED-END ROTATION

One important advantage of the discontinuous slip across elements in the MF formulation is its ability to estimate tbe concrete crack width at the tension side of a cross-section. With the slip u_b equal to the difference between the steel displacement u_s and the concrete displacement u_c, i.e. $u_b = u_s - u_c$, and assuming no rupture in steel reinforcement, the jump in u_b equals the jump in u_c but with opposite sign: $[\![u_b]\!] = -[\![u_c]\!]$, where the jump operator $[\![\cdot]\!]$ is defined as $[\![\cdot]\!] = (\cdot)(x^+) - (\cdot)(x^-)$.

From the values of $[\![u_b]\!]$ for all rebars in an RC cross-section, a crack opening profile can be computed, as shown in Fig. 6 for the preceding numerical analysis results for some drift ratio values ranging from 0% to 6%. The crack profiles in Fig. 6 show that the top concrete fiber (at the tension side) begins to crack when the drift ratio is approximately 1%, and the crack grows rapidly when the drift ratio reaches 4%.

Concrete cracking at member ends results in an additional *fixed-end rotation*. This fixed-end rotation can be estimated from the crack opening profile by fitting a straight line in the form of a crack plane to the slip profile and determining the rotation of this plane relative to the undeformed section. Fig. 6 shows these fitted crack planes for the crack opening profiles of the preceding numerical analysis. With the estimated fixed-end rotation, the relationship between the base moment and the fixed-end rotation at the column base can also be established, as shown in Fig. 6. The moment-rotation relationships in Fig. 6 show that the RC column starts to lose strength when the fixed-end rotation approaches 0.005 rad.

CONCLUSIONS

This paper proposes a composite frame element for the simulation of the inelastic response of structural members made up of two or more components with different materials accounting for the relative slip at the interface between components. Application examples include reinforced concrete members with bond-slip of reinforcing steel, steel-concrete composite members with slip at the interface, members with FRP reinforcement, and prestressed concrete and timber members with partially bonded straight tendons.

The proposed frame element introduces one additional degree of freedom at each node to represent the relative slip of a component relative to the reference component. These slip DOFs rotate with the tangent at the element node so that the slip DOF increments during the iterative solution of the global equilibrium equations can be solved in the local reference system. This holds true even under nonlinear geometry as long as the co-rotational formulation is used for large displacement analysis, making the proposed frame element with slip DOFs easy to implement in a general purpose finite element analysis program for large displacement analysis, a feature that distinguishes this element from earlier proposals.

The study presents three alternative mixed formulations for the composite frame element by enhancing the standard Hu-Washizu variational principle with additional fields for the bond-slip at the interface between components. These formulations are a mixed-displacement (MD), a mixed-force (MF), and a mixed-mixed (MM) formulation. The MD formulation interpolates the slip distribution between components, the MF formulation interpolates the force distribution of components that slip relative to the reference component, and the MM formulation interpolates both slip and force distributions.

To balance interpolation accuracy for the relative slip and the axial force distribution for a component that slips relative to the reference component with interpolation efficiency for the total section forces N and M of the element with the smallest number of parameters, piecewise polynomials for the interpolation of the force and slip distributions at the interface between components are used in the study.

All three formulation alternatives ensure the exact interpolation of the total section force fields for the composite frame element, a feature that distinguishes this element from earlier proposals.

Both MD and MM formulations enforce slip continuity but relax the force continuity, while the MF formulation enforces force continuity but relaxes the slip continuity at the common node of two elements.

Large cracks that form between structural members as a result of relative slip of constituent components require that the slip across the crack at a common node of two elements be discontinuous, while the stress field be continuous. Because the MF formulation captures both phenomena, whereas the MD and MM formulations do not, it is the most suitable for representing the pull-out of reinforcing steel from an anchoring element and determining the resulting fixed-end rotation at the interface between adjacent elements, as demonstrated with the example of a reinforced-concrete cantilever column.

The numerical convergence behavior and the accuracy of the proposed formulations in simulating the global and local response of a steel-concrete composite specimen, and two reinforced-concrete cantilever column specimens with pull-out from the foundation are presented in the companion paper.

REFERENCES

Ayoub, A. and Filippou, F. C. (2000). "Mixed formulation of nonlinear steel-concrete composite beam element." *Journal of Structural Engineering*, 126(3), 371–381.

Ayoub, A. S. (1999). "Mixed formulation for seismic analysis of composite steel-concrete frame structures." Ph.D. thesis, University of California, Berkeley.

Ayoub, A. S. (2006). "Nonlinear analysis of reinforced concrete beam-columns with bond-slip." *Journal of Engineering Mechanics*, 132(11), 1177–1186.

Ayoub, A. S. and Filippou, F. C. (1999). "Mixed formulation of bond slip problems under cyclic loads." *Journal of Structural Engineering*, 125(6), 661–671.

Bousias, S. N., Verzeletti, G., Fardis, M. N., and Gutierrez, E. (1995). "Load-path effects in column biaxial bending with axial force." *Journal of Engineering Mechanics*, 121(5), 596–605.

Coleman, J. and Spacone, E. (2001). "Localization issues in force-based frame elements." *Journal of Structural Engineering*, 127(11), 1257–1265.

Dall'Asta, A. and Zona, A. (2002). "Non-linear analysis of composite beams by a displacement approach." *Computers & Structures*, 80(27-30), 2217–2228.

Dall'Asta, A. and Zona, A. (2004). "Three-field mixed formulation for the non-linear analysis of composite beams with deformable shear connection." *Finite Elements in Analysis and Design*, 40(4), 425–448.

Eligehausen, R., Popov, E. P., and Bertero, V. V. (1983). "Local bond stress-slip relationships of deformed bars under generalized excitations : experimental results and analytical model." *Report No. EERC 83/23*, Earthquake Engineering Research Center, University of California, Berkeley.

Felippa, C. and Haugen, B. (2005). "A unified formulation of small-strain corotational finite elements: I. theory." *Computer Methods in Applied Mechanics and Engineering*, 194(21), 2285–2335.

Filippou, F. C. and Constantinides, M. (2004). "FEDEASLab getting started guide and simulation examples." *Report No. NEESgrid-2004-22*, Dept. of Civil and Environmental Eng., University of California at Berkeley.

Filippou, F. C., D'Ambrisi, A., and Issa, A. (1999). "Effects of reinforcement slip on hysteretic behavior of reinforced concrete frame members." *ACI Structural Journal*, 96(3), 327–335.

Filippou, F. C. and Issa, A. (1988). "Nonlinear analysis of reinforced concrete frames under cyclic load reversals." *Report No. UCB/EERC-88/12*, Earthquake Engineering Research Center, University of California, Berkeley.

Filippou, F. C., Popov, E. P., and Bertero, V. V. (1983). "Effects of bond deterioration on hysteretic behavior of reinforced concrete joints." *Report No. UCB/EERC-83/19*, Earthquake Engineering Research Center, University of California, Berkeley.

Hjiaj, M., Battini, J.-M., and Huy Nguyen, Q. (2012). "Large displacement analysis of shear deformable composite beams with interlayer slips." *International Journal of Non-Linear Mechanics*, 47(8), 895–904.

Le Corvec, V. (2012). "Nonlinear 3d frame element with multi-axial coupling under consideration of local effects." Ph.D. thesis, University of California, Berkeley.

Lee, C. and Filippou, F. (2010). "Mixed formulation for composite and RC frame element with bond-slip." *Structures Congress 2010, 19th Analysis and Computation Specialty Conference*, ASCE, 516–526.

Lee, C.-L. (2008). "Hu-Washizu 3d frame formulations including bond-slip and singular section response." Ph.D. thesis, University of California, Berkeley.

Lee, C.-L. and Filippou, F. C. (2009). "Frame elements with mixed formulation for singular section response." *Int. Journ. Num. Meth. Engrg*, 78(11), 1261–1386.

Limkatanyu, S. and Spacone, E. (2002). "Reinforced concrete frame element with bond interfaces. I: Displacement-based, force-based, and mixed formulations." *Journal of Structural Engineering*, 128(3), 346–355.

Lin, X. and Zhang, Y. (2013). "Novel composite beam element with bond-slip for nonlinear finite-element analyses of steel/FRP-reinforced concrete beams." *Journal of Structural Engineering*, 139(12) 06013003.

Mander, J. B., Priestley, M. J. N., and Park, R. (1988). "Theoretical stress-strain model for confined concrete." *Journal of Structural Engineering*, 114(8), 1804–1826.

Mckenna, F. T. (1997). "Object-oriented finite element programming: frameworks for analysis, algorithms and parallel computing." Ph.D. thesis, University of California, Berkeley.

Menegotto, M. and Pinto, P. E. (1973). "Method of analysis for cyclically loaded reinforced concrete plane frames including changes in geometry and non-elastic behavior of elements under combined normal force and bending." *IABSE Symposium on Resistance and Ultimate Deformability of Structures Acted on by Well Defined Repeated Loads*, Lisbon, 15–22.

Monti, G., Filippou, F. C., and Spacone, E. (1997). "Finite element for anchored bars under cyclic load reversals." *Journal of Structural Engineering*, 123(5), 614–623.

Monti, G. and Spacone, E. (2000). "Reinforced concrete fiber beam element with bond-slip." *Journal of Structural Engineering*, 126(6), 654–661.

Rubiano-Benavides, N. R. (1998). "Predictions of the inelastic seismic response of concrete structures including shear deformations and anchorage slip." Ph.D. thesis, University of Texas, Austin.

Saatcioglu, M., Alsiwat, J. M., and Ozcebe, G. (1992). "Hysteretic behavior of anchorage slip in R/C members." *Journal of Structural Engineering*, 118(9), 2439–2458.

Salari, M. R. and Spacone, E. (2001a). "Analysis of steel-concrete composite frames with bond-slip." *Journal of Structural Engineering*, 127(11), 1243–1250.

Salari, M. R. and Spacone, E. (2001b). "Finite element formulations of one-dimensional elements with bond-slip." *Engineering Structures*, 23(7), 815–826.

Salari, M. R., Spacone, E., Shing, P. B., and Frangopol, D. M. (1998). "Nonlinear analysis of composite beams with deformable shear connectors." *Journal of Structural Engineering*, 124(10), 1148–1158.

Saritas, A. (2006). “Mixed formulation frame element for shear critical steel and reinforced concrete members.” Ph.D. thesis, University of California, Berkeley.

Scott, M. H. and Fenves, G. L. (2006). “Plastic hinge integration methods for force-based beam–column elements.” *Journal of Structural Engineering*, 132(2), 244–252.

Spacone, E. and El-Tawil, S. (2004). “Nonlinear analysis of steel-concrete composite structures: State of the art.” *Journal of Structural Engineering*, 130(2), 159–168.

Spacone, E., Filippou, F. C., and Taucer, F. F. (1996). “Fiber beam-column model for nonlinear analysis of RC frames: I: Formulation.” *Earthquake Engineering and Structural Dynamics*, 25(7), 711–725.

Sun, F.-F. and Bursi, O. S. (2005). “Displacement-based and two-field mixed variational formulations for composite beams with shear lag.” *Journal of Engineering Mechanics*, 131(2), 199–210.

Taylor, R. L., Filippou, F. C., Saritas, A., and Auricchio, F. (2003). “Mixed finite element method for beam and frame problems.” *Computational Mechanics*, 31(1-2), 192–203.

Tort, C. and Hajjar, J. F. (2010). “Mixed finite element for three-dimensional nonlinear dynamic analysis of rectangular concrete-filled steel tube beam-columns.” *Journal of Engineering Mechanics*, 136(11), 1329–1339.

List of Figures

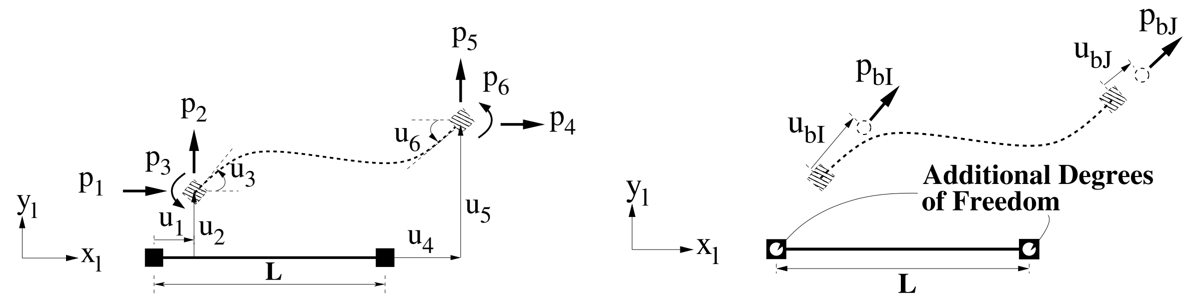

(a) Nodal forces and displacements of standard frame element

(b) Additional nodal forces and displacements for frame element with bond-slip

FIG. 1. Nodal forces and displacements of standard frame element and composite frame element with slip between two components

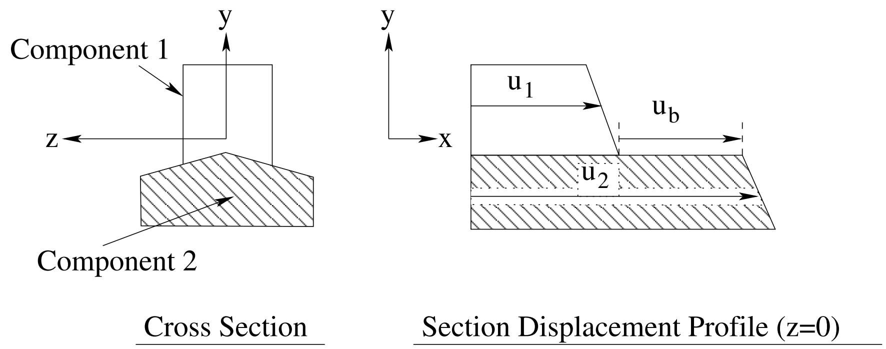

FIG. 2. Section configuration and displacement profile

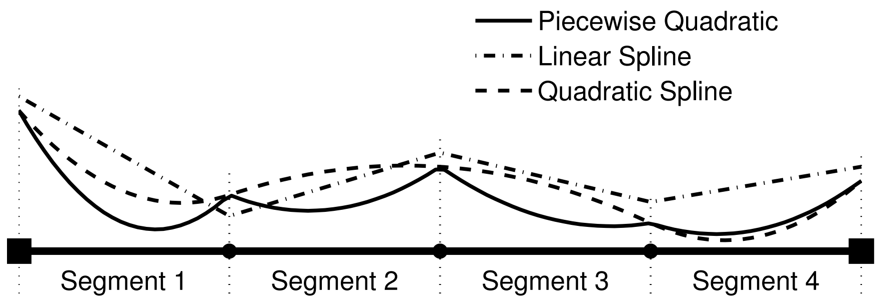

FIG. 3. Examples of interpolation functions

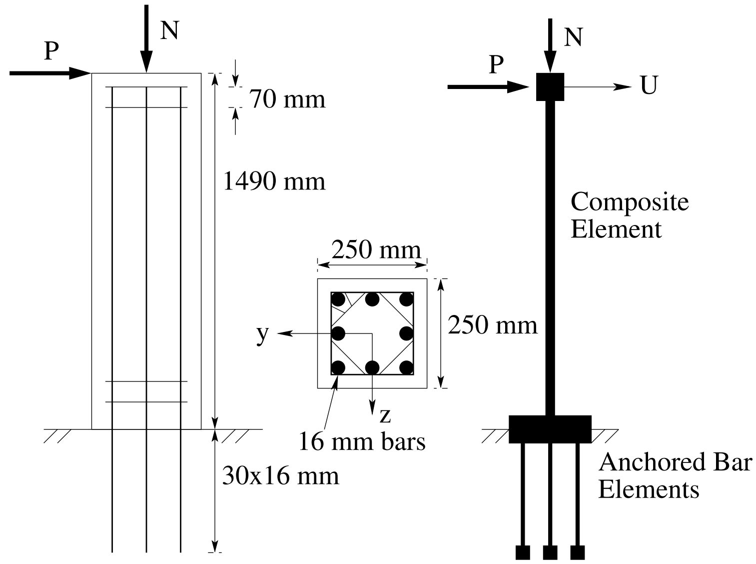

FIG. 4. Reinforced-concrete cantilever column

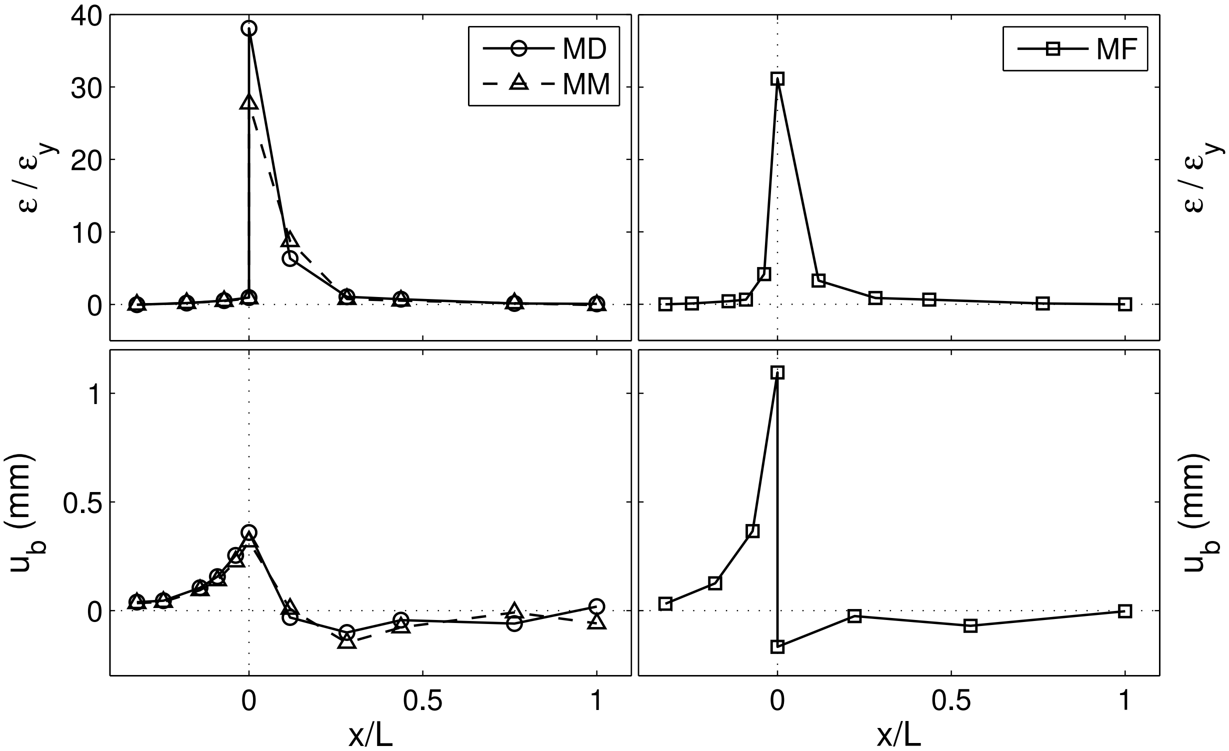

FIG. 5. Strain and slip distributions of steel reinforcing bars in tension at 6% drift ratio

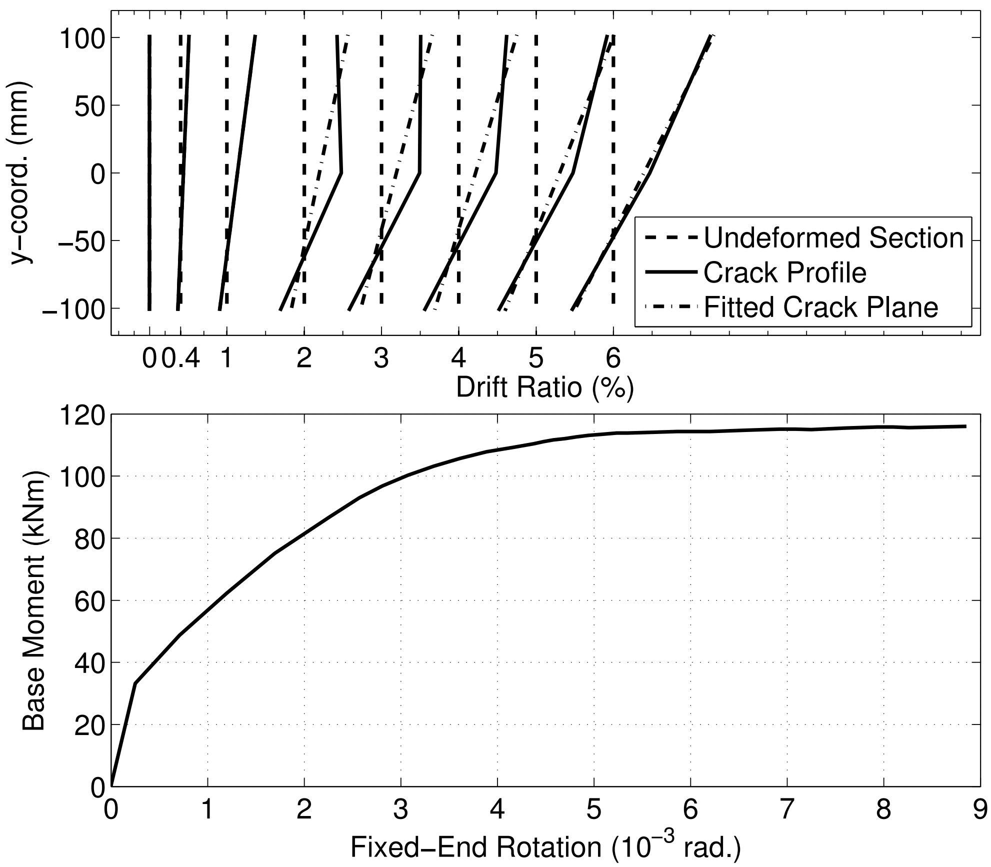

FIG. 6. Crack opening profiles and fitted crack planes for drift ratios of 0%, 0.4%, 1%, 2%, 3%, 4%, 5% and 6%, and moment versus fixed-end rotation at column base